Analytically soluble model for fusion time

V. J. Menon and S. N. Mukherjee
Department of Physics, Banaras Hindu University, Varanasi 221 005, India

C. S. Shastry and B. Sahu
Department of Physics, North-Eastern Hill University, Shillong 793 003, India

(Received 21 March 1989)

We derive an analytical expression for the essential parameters (viz., positions, heights, and curvatures) characterizing the extrema of the effective potential between two heavy ions. These parameters together with the energy are used to calculate, in closed form, the times for complete fusion above the Coulomb barrier. The method is found to work well for nuclear (and/or Coulomb) trajectories of zero or small orbital angular momentum when friction is absent. The inclusion of dissipation is shown to reduce the fusion time substantially for typical heavy-ion systems provided the energy satisfies certain kinematic constraints.

I. INTRODUCTION

The important question of theoretically estimating the time scale T for complete fusion in heavy-ion collisions has been discussed by several workers.[1-5] It is customary to regard T as (i) the duration T_C or T_{CN} spent by the system within the fusion distance R_F while moving on the classical Coulomb[1] (C) or Coulomb-nuclear[2] (CN) trajectory at energy E above the barrier height V_B; (ii) the equilibration[3] time T_e of two deformed interpenetrating Fermi spheres; (iii) the Wigner time delay T_{PS} computed from partial wave phase shifts[4] in a barrier-transmission model both above and below V_B; or (iv) the formation time T_f of the fused system by the barrier tunneling[5] of the incident particle flux at $E < V_B$, etc. Reference 5 also gives an exhaustive numerical comparison of the above-mentioned estimates for T at many energies for typical pairs of nuclei.

The aim of this paper is to incorporate the effect of radial *friction* on the classical CN trajectory model for T at energies above the barrier. The role of friction has been extensively discussed[6] in the past either for computing deep-inelastic and fusion semiclassical *cross sections*,[7] or for probing the nature of quantal *energy dissipation*[8] during fission. Our purpose is to formulate a classical theory of fusion times which is mathematically soluble, physically meaningful, and which resolves the following crucial issues.

(a) For the $E > V_B$ case, the CN trajectory time T_{CN} is usually evaluated[5] through an elaborate numerical quadrature whose integrand depends upon the detailed knowledge of the total potential $V_T(R)$ between the ions. The question arises as to which portion (or which parameters) of $V_T(R)$ is T_{CN} really sensitive, and what is the explicit formula for T_{CN} in terms of these parameters when dissipation is absent? This will be answered in Sec. II.

(b) It was found numerically in Ref. 5 that for low-lying orbital angular momenta L much below the grazing value, the output T_{CN} is insensitive to L. We will take up this point also in Sec. II.

(c) In the $E > V_B$ case it is essential to add frictional forces if we want the trajectories to be arrested permanently; a simple model for doing so is the surface-delta term used originally by Bass[9] to explain fusion cross sections. It is relevant to ask how the formula for T_{CN} is altered in the presence of dissipation, and what is the precise kinematic condition for guaranteeing fusion? Section III will examine these issues in detail.

In Sec. IV we will present the numerical results of our theory applied to some interesting heavy-ion systems both without and with friction. Section V discusses the main conclusions of our work. Finally, the appendix lists a set of useful formulas concerning the potential $V_T(R)$ and its derivatives.

II. FORMALISM WITHOUT FRICTION

A. Notation

For the sake of convenience we make the following definitions. (A_1, A_2) denote mass numbers of the colliding nuclei; (Z_1, Z_2) denote their charge numbers; R denotes the interion separation distance; $R_N = R_C = r_0(A_1^{1/3} + A_2^{1/3})$ denotes nuclear or Coulomb radius, both assumed to be equal for simplicity; L denotes the orbital angular momentum; $l = L/\hbar$ denotes the orbital quantum number; m denotes the nucleon mass; $\mu = A_1 A_2 m/(A_1 + A_2)$ denotes the reduced mass of the system; (V_0, r_0, a) denotes the Woods-Saxon parameters; $D_N = V_0/2$; $D_C = Z_1 Z_2 e^2/R_N$; $D_L = L^2/(2\mu R_N^2)$; $Y = (R - R_N)/2a$; $G_0 = (R_N D_N/2aD_C)^{1/2}$; $J_0 = (G_0^2 - 1)^{1/2}$; R_F denotes the fusion distance; and E denotes the incident energy of relative motion.

B. Effective potential

We can write the total potential energy as the sum of the nuclear, Coulomb, and centrifugal parts as

$$V_T(R)=V_N(R)+V_C(R)+V_L(R)\ , \tag{1a}$$

where

$$V_N(R)=-V_0/[1+\exp(R-R_N)/a]$$
$$=-D_N/[e^Y\cosh Y)\ , \tag{1b}$$

$$V_C(R)=0.5D_C(3-R^2/R_C^2),\quad R<R_C$$
$$=D_CR_C/R,\quad R>R_C\ , \tag{1c}$$

$$V_L(R)=L^2/2\mu R^2\ . \tag{1d}$$

A schematic plot of V_T vs R is shown in Fig. 1; algebraic properties of V_T and its derivatives are listed in the appendix.

C. Barrier

The maximum of V_T appears at a point $R_B=R_N+2aY_B$, where Y_B is positive and fulfills the condition [see appendix, Eq. (A4)]

$$\cosh^2Y_B=G_0^2/(1+2D_L/D_C)[1+O(a/R_N)] \tag{2}$$

to lowest order in the ratio a/R_N. The denominator of Eq. (2) is substantially *independent* of L if $2D_L/D_C\ll1$, i.e., if

$$0\le l\le l_B,\quad l_B=(\mu R_N^2D_C/\hbar^2)^{1/2}\ . \tag{3}$$

From Eqs. (2) and (3) we have, for small l,

$$Y_B=(R_B-R_N)/2a=\ln(G_0+J_0)\ , \tag{4}$$

where G_0 and J_0 are defined in subsection A. In the neighborhood of R_B we can expand [cf. Eqs. (A5)–(A7)]

$$V_T(R)=V_B-\tfrac{1}{2}\mu w_B^2x^2\ , \tag{5a}$$

where

$$V_B=D_C\left[1-\frac{2a}{R_N}[Y_B+G_0(G_0-J_0)]\right]\ ,$$
$$w_B=(D_CJ_0/\mu aR_NG_0)^{1/2},\quad x=R-R_B\ . \tag{5b}$$

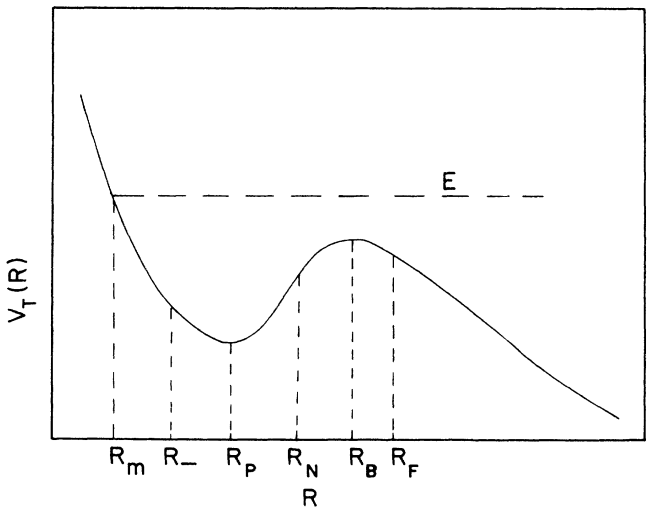

FIG. 1. A schematic plot of the effective potential V_T vs the internuclear separation R. Various points of physical interest have been marked. E indicates typical incident energy.

D. Pocket

Next, the minimum of V_T appears at a point $R_p=R_N+2aY_p$, where Y_p is negative and fulfills the same condition as Eq. (2). Hence, to leading order in the ratio a/R_N we have

$$Y_p=(R_p-R_N)/2a=\ln(G_0-J_0)\ . \tag{6}$$

In the neighborhood of R_p the potential is again represented by the parabola

$$V_T(R)=V_P+\tfrac{1}{2}\mu w_p^2y^2\ , \tag{7a}$$

where, in close analogy with Eq. (5b),

$$V_p=D_C\left[1-\frac{2a}{R_N}[Y_p+G_0(G_0+J_0)]\right]\ ,$$
$$w_p=w_B,\quad y=R-R_p\ . \tag{7b}$$

What is the range of validity of our approximations leading to Eqs. (2)–(7b)? Since we have treated a/R_N as a perturbation parameter (which typically is of order $\frac{1}{20}$), we expect the resulting values of R_B and R_p to be correct to within about 5% or better. Next, the reality of J_0 requires $G_0>1$. Also, the condition that R_B and R_p should both be close to R_N implies that $|Y_B|=|Y_P|\ll R_N/2a$ in Eqs. (4) and (6), i.e.,

$$G_0>1,\quad \ln(G_0+J_0)\ll R_N/2a\ . \tag{7c}$$

This inequality is well satisfied for most heavy-ion systems of interest, e.g., $G_0=1.75$, $\ln(G_0+J_0)=1.16$, and $R_N/2a=19$ in the case of ^{58}Ni+^{124}Sn. However, if G_0 becomes too large, i.e., the Woods-Saxon parameter is excessively deep, our approximations would cease to be valid.

E. Closest approach

In the absence of dissipative forces, both E and L are conserved. The radial velocity vanishes at a point R_m such that $V_T(R_m)=E$. Within the nuclear interior, $V_N(R)$ can be replaced by $-V_0$, and for low angular momenta, $V_L(R)$ may be neglected in Eqs. (1a)–(1d). Therefore, the turning points in the Coulomb-nuclear (CN) and pure Coulomb (C) cases are given, respectively, by

$$R_m^{\rm CN}=[2(1.5D_C-2D_N-E)/\mu w_m^2]^{1/2}\ ,$$
$$R_m^{C}=[2(1.5D_C-E)/\mu w_m^2]^{1/2}\ , \tag{8a}$$

$$w_m=[(D_C/\mu R_N^2)]^{1/2}\ . \tag{8b}$$

For $L>0$ the corresponding distance of closest approach denoted by $R_m^{\rm CN}(L)$ increases quite slowly with L, as seen from the expression

$$[R_m^{\mathrm{CN}}(L)]^2=(R_m^{\mathrm{CN}})^2 \times\{1+\mu w_m^2 D_L/[2(1.5D_C-2D_N-E)] +\cdots\}\ . \tag{8c}$$

In the *inner* region we can approximate

$$V_T(R)=\tfrac{3}{2}D_C-2D_N-\tfrac{1}{2}\mu w_m^2 R^2\ . \tag{9}$$

F. Regions

Equations (5a), (7a), and (9) express the potential in a simple algebraic form in the barrier, pocket, and turning point regions, respectively. Various parameters appearing therein are of crucial importance because, as will be demonstrated in Sec. III, they govern the temporal dynamics of complete fusion. In what follows we assume that $G_0>1$, so that J_0 is positive and $R_N<R_B<R_F$, which is usually the case in practice. Initially, at the instant zero, the system was supposed to be just crossing the fusion distance R_F with a negative velocity $\dot{R}_F$ (the overdot representing the time derivative), i.e.,

$$R=R_F=R_B+x_F\ , \qquad \dot{R}=\dot{R}_F=\dot{x}_F<0 \text{ at } t=0\ . \tag{10}$$

G. Coulomb time

For the sake of ready reference we first quote the formula for time scales in the case of Coulomb trajectories with $L=0$ and $V_C(R)$ given by Eq. (1c). The duration $T_C^{>}$ needed by the system to go from R_F to R_C is

$$T_C^{>}=H[I(z_F)-I(z_C)]\ , \tag{11a}$$

where

$$H^2=\mu R_C^2 D_C^2/2E^3,\quad z_F^2=R_F E/R_C D_C\ , \qquad z_C^2=E/D_C,\quad I(z)=z(z^2-1)+\cosh^{-1}z\ . \tag{11b}$$

Also, motion from R_C to R_m^C [cf. Eq. (8)] occurs during the interval

$$T_C^{<}=\cosh^{-1}(R_C/R_m^C)/w_m\ . \tag{12}$$

The required fusion time is computed from

$$T_C=2(T_C^{>}+T_C^{<})\ . \tag{13}$$

However, numerical results on the Coulomb time will not be reported in this paper, as those have been discussed in Refs. 1 and 5.

H. Coulomb-nuclear time

Next, we consider a trajectory with $L=0$ under the potential $V_T(R)$ [cf. Eq. (5)] in the barrier region $R_N<R<R_F$. The Newtonian equation of motion $\ddot{x}-w_B^2 x=0$ subjected to the initial condition (10) has the solution

$$x=R-R_B=-b\sinh(w_B T-\phi_B)\ , \tag{14a}$$

with

$$b=\left[\frac{2(E-V_B)}{\mu w_B^2}\right]^{1/2},\quad \phi_B=\sinh^{-1}\frac{|x_F|}{b}\ . \tag{14b}$$

The system reaches the point $R=R_N$, i.e., $x=x_N$ after the time duration T_+ given by

$$T_+=\frac{1}{\omega_B}\left[\sinh^{-1}\frac{|x_N|}{b}+\phi_B\right]\ . \tag{15}$$

Thereafter motion starts in the *pocket* region $R_-=2R_p-R_N<R<R_N$ described by the potential $V_T(R)$ [cf. Eq. (7) and Fig. 1]. Newton's law $\ddot{y}+w_P^2 y=0$ is integrated to yield the trajectory

$$y=R-R_p=p\cos[w_p(t-T_+)+\phi_p]\ , \tag{16a}$$

with

$$p=\left[\frac{2(E-V_P)}{\mu w_p^2}\right]^{1/2},\quad \phi_p=\cos^{-1}\frac{y_N}{p}\ . \tag{16b}$$

The left edge R_- of the pocket is reached after a further time lapse T_p such that

$$T_p=(\pi-2\phi_p)/w_p\ . \tag{17}$$

Upon leaving the pocket the system enters the *inner* region $R_m^{\mathrm{CN}}<R<R_-$ described by the potential $V_T(R)$ [cf. Eq. (9)]. The equation of motion $\ddot{R}-w_m^2 R=0$ leads to the solution [cf. Eq. (8)]

$$R=R_m^{\mathrm{CN}}\cosh[\phi_- -w_m(t-T_+-T_p)]\ . \tag{18}$$

The phase ϕ_- and the additional time interval T_- needed to reach the distance of closest approach are obtained from

$$\phi_-=\cosh^{-1}(R_-/R_m^{\mathrm{CN}}),\quad T_-=\phi_-/w_m\ . \tag{19}$$

Taking into account the return journey from R_m^{CN} back to R_F we get the desired time scale for fusion in the absence of dissipation as

$$T_{\mathrm{CN}}=2(T_+ +T_p+T_-)\ . \tag{20}$$

Clearly, T_{CN} is crucially controlled by the energy E as well as the parameters characterizing the barrier, pocket, and inner domains of $V_T(R)$.

III. INCLUSION OF FRICTION

A. Equation of motion

Phenomenologically, the radial friction force between two nuclei is written as

$$F=-Qf(R)\dot{R}\ , \tag{21}$$

where Q is a positive coefficient, $f(R)$ a geometrical form factor, and $\dot{R}$ the relative radial velocity. For low-lying partial waves $l\ll l_B$ [cf. Eq. (3)] the motion is essentially one-dimensional, so that *tangential* friction need not be considered. In the literature several possible models for $f(R)$ exist, e.g., the surface-delta form of Bass,[9] the

proximity-window term of Randrup,[10] the double-derivative model of Gross,[11] and the overlap-volume ansatz of Wilczynska *et al.*[12] All these choices (except the first) require heavy computational labor during application to deep-inelastic and/or fusion cross sections. In this paper we take the Bass model $f(R)=\delta(R-R_N)$ which is known to fit cross-section data reasonably well. Newton's equation now reads

$$\mu\frac{d^2R}{dt^2}=-\frac{d}{dR}V_T(R)-Q\frac{d}{dt}\Theta(R-R_N)\ , \tag{22}$$

where Θ is the step function.

B. Integration

Define an infinitesimally small time interval T_+-0 to T_++0 during which the system crosses the point R_N where T_+ is read off from Eq. (15). Integrating Eq. (22) with respect to t over this interval and remembering that dV_T/dR is continuous in R, we obtain

$$\dot{R}(T_++0)-\dot{R}(T_+-0)=-Q/\mu\ . \tag{23}$$

Thus the *speed* $\dot{R}$ drops by an amount Q/μ every time the nuclear edge is crossed. To keep track of the pattern of energy loss, it is convenient to introduce the symbols

$$\begin{aligned}|\dot{R}_N|&=\{2[E-V_T(R_N)]/\mu\}^{1/2}\ ,\\ E^{(n)}&=\tfrac{1}{2}\mu(|\dot{R}_N|-nQ/\mu)^2+V_T(R_N)\ .\end{aligned} \tag{24}$$

Here $|\dot{R}_N|$ was the speed just before the *first* crossing of the nuclear edge, $V_T(R_N)=D_C-D_N$ is the effective potential there, and n is the number of crossings which have taken place.

C. Temporal evolution

In the first stage the system moves from R_F to R_N during $0<t<T_+$ [cf. Eq. (15)] at incident energy $E^{(0)}=E$ without friction. In the next stage the movement occurs from R_N to the turning point and back during

$$T_+<t<T_++2(T_P^{(1)}+T_-^{(1)})\ ,$$

where $T_P^{(1)}$ and $T_-^{(1)}$ are the same as T_P and T_-, respectively [cf. Eqs. (17) and (19)], but evaluated at a smaller energy $E^{(1)}$ due to friction. In the final stage the system will either go towards R_F by overcoming the barrier if $E^{(2)}>V_B$, or get permanently trapped below the barrier if $E^{(2)}<V_B$.

D. Fusion criterion

In order that the colliding classical heavy-ion system overcomes the barrier, it is essential that the initial energy $E^{(0)}>V_B$, i.e., $|\dot{R}_N|>v_0$, where

$$v_0=[2(V_B-D_C+D_N)/\mu]^{1/2}\ . \tag{25}$$

Also, for trapping the system permanently the energy $E^{(2)}$ of Eq. (24) must become less than the barrier height, i.e., $|\dot{R}_N|-2Q/\mu<v_0$. Hence the algebraic criterion for complete fusion is

$$V_B<E<\left[\tfrac{1}{2}\mu\left[v_0+\frac{2Q}{\mu}\right]^2+D_C-D_N\right]\ . \tag{26}$$

Note that the upper limit here depends on the value of Q.

E. New fusion time

Given the condition (26), the fusion time $\bar{T}_{\rm CN}$ under friction becomes simply the old passage time T_+ from R_F to R_N without dissipation, i.e.,

$$\bar{T}_{\rm CN}=T_+<T_{\rm CN}\ , \tag{27}$$

where $T_{\rm CN}$ is read off from Eq. (20). We observe the important property that $\bar{T}_{\rm CN}$ is *independent* of Q and is substantially less than $T_{\rm CN}$.

F. Coefficient of friction

Originally Bass[9] had taken $Q\to\infty$ so that the kinetic energy may drop to zero immediately after the system enters the nuclear radius. However, since we need a finite Q, the following *optimum* choice is made: If the incident energy were equal to the barrier height, the speed after two crossings just vanishes, i.e.,

$$v_0-2Q/\mu=0,\quad Q=\mu v_0/2\ . \tag{28}$$

Substituting for Q in Eq. (26) we get a very simple fusion condition

$$V_B<E<4V_B-3(D_C-D_N)\ . \tag{29}$$

IV. NUMERICAL RESULTS

We shall now apply the above-mentioned theory to some typical heavy-ion systems considered also by Sahu and Shastry.[5] Table I gives the relevant nuclear optical potential parameters[2,5] (regarded as real and energy independent) along with the nuclear radii R_N and fusion distances R_F. Table II displays the corresponding values

TABLE I. Optical potential parameters (V_0,r_0,a), nuclear radius R_N, and fusion distance R_F for selected (heavy-ion) pairs taken from Ref. 5.

System	V_0 (MeV)	r_0 (fm)	a (fm)	R_N (fm)	R_F (fm)
^{40}Ar+^{122}Sn	41.8	1.25	0.51	10.47	12.57
^{81}Br+^{90}Zr	35.0	1.35	0.43	11.89	12.42
^{58}Ni+^{64}Ni	40.0	1.25	0.55	9.84	11.41
^{58}Ni+^{124}Sn	58.1	1.26	0.294	11.16	12.58

TABLE II. Theoretical values of the barrier and pocket parameters for $l=0$ as deduced from our approximate analytical formulas [(4), (5b), (6), and (7b)]. The entries in parentheses are obtained from the exact numerical plot of the total potential V_T.

System	R_B (fm)	V_B (MeV)	$\omega_B=\omega_P$ (c/fm)	R_P (fm)	V_P (MeV)
$^{40}Ar+^{122}Sn$	11.27	107.1	0.0231	9.68	98.59
	(11.39)	(107.8)	(0.021)	(9.79)	(99.24)
$^{81}Br+^{90}Zr$	12.42	154.1	0.0213	11.36	150.0
	(12.49)	(154.4)	(0.020)	(11.42)	(150.3)
$^{58}Ni+^{64}Ni$	10.60	97.86	0.0211	9.08	91.65
	(10.75)	(98.61)	(0.0190)	(9.20)	(92.25)
$^{58}Ni+^{124}Sn$	11.84	164.4	0.0349	10.48	138.8
	(11.88)	(165.0)	(0.0323)	(10.52)	(139.45)

of the barrier and pocket parameters $R_B, V_B, W_B = W_P, V_P$ for $l=0$ as derived from our approximate analytical formulas [cf. Eqs. (4), (5b), (6), and (7b)]—these values compare well with those obtained from the exact *numerical* plot of the effective potential V_T vs R (the entries in parentheses in Table II).

In the following calculations the fusion times will always be calculated within the energy range $V_B < E < 4V_B - 3(D_C - D_N)$ as suggested by Eq. (29); consider first the case when there is *no* dissipation so that our Eqs. (15), (17), (19), and (20) are applicable for determining T_+, T_P, T_-, and T_{CN}, respectively. In the specific case of the $^{58}Ni+^{124}Sn$ system, Table III gives the explicit values of these times (as a function of energy) as calculated from

TABLE III. Explicit values of the various components of fusion time without dissipation as predicted by our theory [cf. Eqs. (15)–(20)] for the illustration case of $^{58}Ni+^{124}Sn$. Entries in parentheses are obtained from numerical integration over the relevant portions of the classical trajectory.

E (MeV)	T_+ (fm/c)	T_P (fm/c)	T_- (fm/c)	T_{CN} (fm/c)
168.25	75.06	36.56	110.73	444.70
	(81.76)	(33.85)	(108.2)	(447.7)
172.10	58.76	34.08	122.31	430.29
	(61.55)	(31.59)	(120.5)	(427.2)
175.94	50.17	32.04	134.22	432.87
	(51.73)	(29.74)	(130.4)	(423.6)
179.78	44.59	30.34	146.68	443.19
	(45.56)	(28.18)	(141.4)	(430.3)
183.63	40.56	28.88	159.96	458.78
	(41.20)	(26.84)	(161.8)	(459.7)
187.47	37.47	27.61	174.41	478.97
	(37.91)	(25.68)	(170.4)	(467.9)
191.31	34.99	26.50	190.51	504.02
	(35.31)	(24.66)	(194.4)	(508.8)
195.16	32.96	25.51	209.03	535.01
	(33.18)	(23.76)	(207.4)	(528.7)
199.0	31.25	24.63	231.26	574.27
	(31.39)	(22.94)	(234.4)	(577.4)
202.84	29.78	23.83	259.73	626.68
	(29.87)	(22.21)	(251.3)	(606.8)

our *analytical* formulas—the same quantities computed from exact *numerical* integration over the relevant trajectories are shown by entries in parentheses in the table. The agreement of the results from these two approaches is quite satisfying.

Next, Fig. 2 displays the energy variation of T_{CN} (solid lines) as predicted by our analytical formula (20) for four pairs of nuclei—the same quantity calculated in Ref. 5 using numerical integration is indicated by points. The agreement is quite good in three of the cases considered, but not for $^{81}Br+^{90}Zr$ (although the trend of T_{CN} vs E is correct, and the *relative* discrepancy does not exceed about 10–20% even in this case). We analyze the origin of this discrepancy in the results obtained by the analytical method and numerical calculations in the case of $^{81}Br+^{90}Zr$ as follows: In this case the total potential (Coulomb plus nuclear) with $L=0$ at origin is $V_0=219$ MeV, whereas our time calculation was done in the energy range 154–160 MeV. This large gap between V_0 and energy used makes the turning point occur, in the analytical formulation, very close to R_-. However, the turning point R_m^{CN} in the analytical formula will be somewhat more erroneous in the neighborhood of R_- due to the approximation made that the nuclear potential is constant for $r<R_-$. Now we notice that $\cosh^{-1}(x)$, $x\gtrsim 1$, is a very rapidly increasing function of x in the neighborhood of $x=1$, its slope being infinity at $x=1$. Hence, a minor error in R_m^{CN} can cause a major change in $\cosh^{-1}(R_-/R_m^{CN})$, and hence a somewhat more serious error in T_-. In the case of three other systems, R_m^{CN} occurs further in the interior close to the origin, and the error caused in R_m^{CN} is negligible. Thus we observe that whenever the turning point R_m^{CN} occurs closer to R_-, i.e., close to the surface region, one can expect a significant error in T_- and hence in $T_{CN}=2(T_-+T_p+T_+)$.

Now, we come to the case when friction *is* present so that the relevant fusion time is simply $\bar{T}_{CN}=T_+$ [cf. Eq. (27)]. The energy variation of $\bar{T}_{CN}$ as predicted by our analytical formula (15) is shown graphically by solid lines in Fig. 3, which also includes the T_+ values obtained from numerical quadrature (see the points). The comparison is again fairly good to within about 5%. It should be emphasized that $\bar{T}_{CN}$ is about 4 to 8 times smaller than T_{CN}, i.e., friction reduces the fusion times substantially. The physical reason behind such a marked difference between the results of Figs. 2 and 3 is linked to the fact that, in the absence of friction, there are *four* main portions of the trajectory to be covered, viz., R_F to R_N, R_N to R_m, R_m to R_N, and R_N to R_F back (cf. Fig. 1). However, when dissipation is operative, only *one* portion of the trajectory, viz., R_F to R_N, is relevant as far as the fusion time is concerned. Naturally, T_{CN} will be much larger than $\bar{T}_{CN}$.

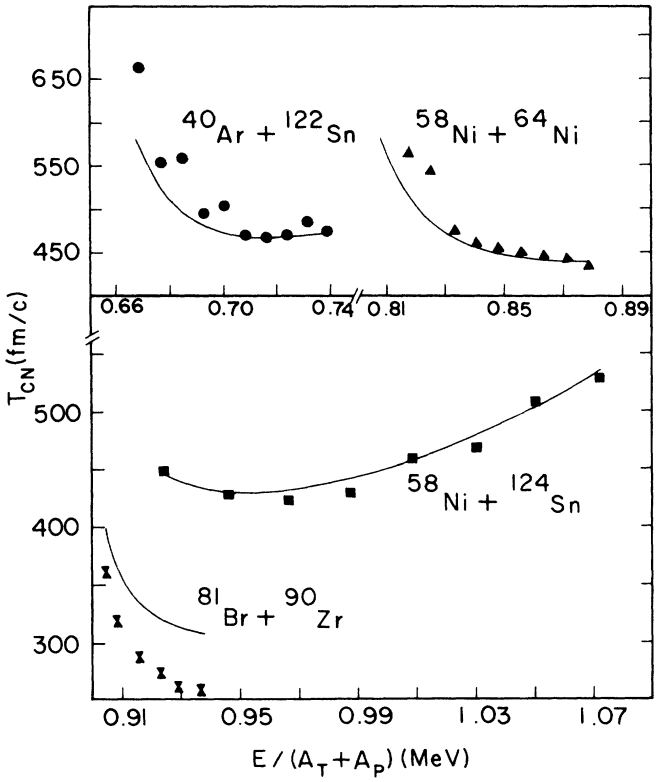

FIG. 2. The energy variation of the fusion time in the absence of friction for four pairs of nuclei. The solid lines are our predictions according to Eq. (20). The results indicated by points are based on numerical quadrature as done in Ref. 5.

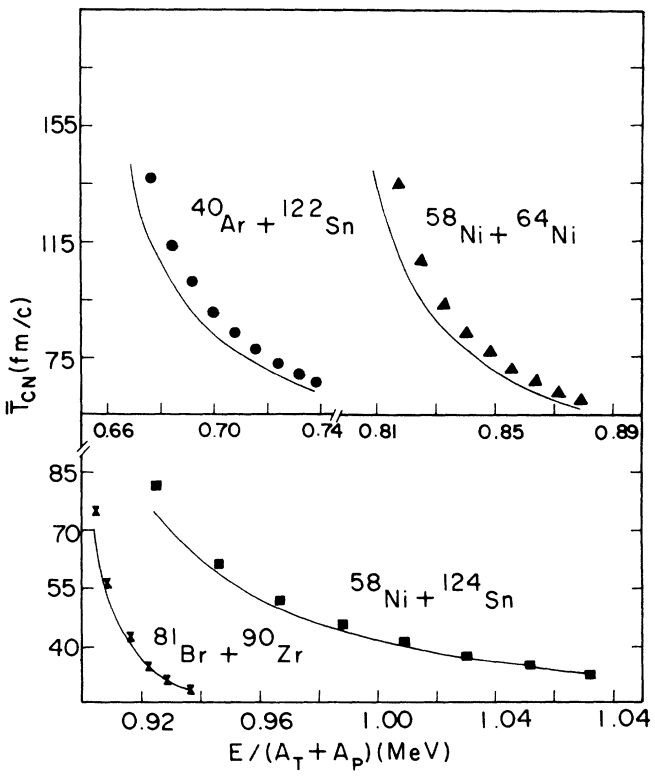

FIG. 3. The energy variation of the fusion time in the presence of friction for four pairs of nuclei. The solid lines are our predictions according to Eq. (27). The points represent the T_+ values obtained by numerical quadrature.

Finally, a few words about the coefficient of friction Q for which a plausible choice was made in Eq. (28). We note that Q does not effect the value T_+ of the new fusion time, so that the results of Fig. 3 are independent of Q. However, the kinematic condition (26) for fusion to occur as well as the pattern of energy loss $E^{(n)}-E^{(0)}$ for the arrested trajectory are sensitive to the choice of Q. Consider, for example, the ^{58}Ni+^{124}Sn system and let $Q=\mu v_0$, $\mu v_0/2$, and $\mu v_0/4$ in succession. We find that the corresponding kinematic domains for incident energy (in MeV) become

$$164.4 < E < (266.9, 202.8, 180.4) . \quad (30)$$

The optimum value 202.8 MeV was used to truncate the energy axes in Figs. 2 and 3 for the ^{58}Ni+^{124}Sn system.

V. DISCUSSION

In this paper we have attempted to formulate a soluble model for fusion times using classical trajectories above the Coulomb barrier. It is worth critically examining the various assumptions that have gone into our work.

Firstly, the use of *classical* dynamics is justified because the de Broglie wavelength of the colliding ions is small compared to the sum of their radii. Secondly, employing a *real* total potential (1) is reasonable because we want real trajectories; introducing a complex optical potential to take into account the quantum-mechanical loss of flux is not of interest here. Thirdly, the assumed *inequality* $R_N < R_B < R_F$ [cf. the paragraph following Eq. (9)] holds for most of the heavy-ion pairs considered in Ref. 5; exceptions such as ^{40}Ca+^{40}Ca (for which $R_N < R_F < R_B$) are few, and one can develop a formalism similar to Secs. II and III to deal with these cases also. Fourthly, although nuclear friction, in general, consists of both the *radial* and *tangential* components, the neglect of the latter is justified in our work because we consider fusion only for small angular momentum $l \approx 0$; then the motion is effectively one-dimensional and radial friction dominates the process of energy dissipation. Fifthly, although actual nuclei do not have sharp edges, and the loss of energy may be *gradual*, yet the use of a Bass[9] type of frictional force [cf. Eq. (22)] may not be a bad approximation because of the following reasons: (i) workers such as Gross[11] have favored a surface-peaked form factor $f(R)$; (ii) the delta-function model is neatly soluble, unlike the other choices of $f(R)$ which require heavy computational labor; and (iii) the substantial reduction of the fusion time from $T_{\rm CN}$ [Eq. (20)] to T_+ [Eq. (27)] is a general feature holding irrespective of the detailed shape of $f(R)$.

Let us now summarize the main conclusions of this paper, keeping in mind also the following three questions raised in Sec. I.

(a) Apart from energy E the quantities which crucially control the fusion time are the parameters (R_B, V_B, w_B), (R_P, V_P, w_P), and $(R^{\rm CN}, w_m)$ characterizing, respectively, the barrier, pocket, and inner regions of the total potential [cf. Eq. (1)] shown in Fig. 1. Our analytical expressions for these parameters derived in Sec. I predict numbers which compare well with their exact numerical values as shown in Table II. Furthermore, the explicit formula for $T_{\rm CN}$ in the absence of dissipation is Eq. (20); it predicts numbers for various heavy-ion pairs which are in good agreement with those[5] obtained by numerical quadrature as depicted in Table III and Fig. 2. Note that the $T_{\rm CN}$ values plotted vs E exhibit a minimum in many cases. The origin of the 10–20% discrepancy observed in the case of ^{81}Br+^{90}Zr in Fig. 2 have been attributed to the error in estimating $R_m^{\rm CN}$ when

$$R_m^{\rm CN} \approx R_- .$$

(b) It is found in Ref. 5 that $T_{\rm CN}$ is quite insensitive to variation in L. This is true as long as the inequality $0 \le l/l_B \le 1$ is fulfilled, where l_B is read off from Eq. (3) (e.g., $l_B = 146$ in the case of the Ni+Sn system). The physical reasons for such a feature are (i) the barrier position R_B diminishes quite slowly with L [Eq. (2)]; (ii) $R^{\rm CN}(L)$ increases slowly with L [Eq. (8c)]; and (iii) V_B increases very slowly with L. The increase in $T_{\rm CN}$ due to (iii) is substantially canceled by the decrease in $T_{\rm CN}$ due to (i) and (ii).

(c) Employing a radial friction force proportional to $\delta(R-R_N)$ we deduce the new fusion time [Eq. (27)] as well as a kinetic condition (29) on the energy. Both these results are worth commenting upon. It is clear from Eq. (27) and Fig. 3 that $\bar{T}_{\rm CN}$ is smaller than $T_{\rm CN}$ by factors like $\frac{1}{4}$ to $\frac{1}{8}$, i.e., friction reduces the fusion time substantially. The physical reason for this observation is the drastic reduction in the length of the trajectory to be covered when dissipation is present. Note that this result is essentially independent of the detailed value of the form factor $f(R)$ in Eq. (22) because fusion, in our viewpoint, will occur once the energy drops below the barrier height so that only the passage time from R_F to R_N is relevant. However, the kinematic condition (29) is very much model *dependent* and sensitive to the choice of the coefficient of friction, as seen from the example in Eq. (30).

We also wish to point out that an alternative viewpoint of fusion could be the formation of a final residual nucleus (e.g., $^{58}_{28}$Ni+$^{124}_{50}$Sn forming $_{78}$Pt as residue). This would imply the colliding trajectories to come completely to rest so that the involved time would be much *larger* than T_+. This viewpoint has not been adopted in this paper, as the pattern of progressive energy loss calculated from $E^{(0)}-E^{(n)}$ [cf. Eq. (24)] is highly model dependent.

Before concluding, it is desirable to briefly summarize the importance of time scales like $T_{\rm CN}$ involved in the heavy-ion collision processes. It is known that in the Fokker-Planck equations which determine the probability distribution of macroscopic variables, the relative motion enters via the interaction time.[13] In this formulation, interaction time is an essential input for the determination of the different transport coefficients. Furthermore, it has been observed that the question of different collective degrees of freedom that influence the fusion cross section depends, among other things, on the time scale of the fusion process.[4] Another important time scale involved in heavy-ion collision is the equilibration time of the compound nucleus[3] estimated using statistical

considerations. We believe a comparative study of such equilibration time and T_{CN} is important in understanding different competing processes like fusion, deep-inelastic collision, direct reaction, etc., in heavy-ion collision. Based on these ideas, a model for the description of the fusion cross section at high energy is developed.[14] Finally, it may be mentioned that the physical quantities like orbital angular momentum, distance of closest approach, interaction time, and equilibration time, even though they may not be directly observable, play an important role in the theoretical interpretation of the nucleus-nucleus collision data.[15]

ACKNOWLEDGMENTS

One of us (V.J.M.) is grateful to the University Grants Commission for the award of a Research Scientist A position. The financial assistance from the Department of Atomic Energy, India is gratefully acknowledged by S.N.M. The authors thank their respective institutes for facilitating this collaborative work.

APPENDIX: THE POTENTIAL AND ITS DERIVATIVES

Let us recall the notation in Sec. II and the expressions (1a)–(1d) for the potential energy. Denoting the derivatives with respect to R by primes, we readily verify that

$$V_N'(R)=D_N/[2a\cosh^2 Y)\ , \tag{A1}$$

$$V_N''(R)=-D_N\sinh Y/(2a^2\cosh^3 Y)\ . \tag{A2}$$

The barrier position R_B is a bit larger than R_N such that

$$V_T'(R_B)=D_N/(2a\cosh^2 Y_B)-D_C R_N/R_B^2 -2D_L R_N^2/R_B^3=0\ , \tag{A3}$$

which implies

$$\cosh^2 Y_B=\frac{G_0^2 R_B^2/R_N^2}{1+2D_L R_N/D_C R_B}\ . \tag{A4}$$

To lowest order in the ratio a/R_N we can replace R_B by R_N on the right-hand side of (A4). Around the point R_B we have the Taylor expansion for $L\approx 0$ as

$$V_T(R)=V_T(R_B)+\tfrac{1}{2}V_T''(R_B)(R-R_B)^2\ , \tag{A5}$$

where, say,

$$V_T(R_B)=\frac{D_C R_N}{R_N+2aY_B}-D_C\frac{2a}{R_N}\frac{G_0}{G_0+J_0}\equiv V_B\ , \tag{A6}$$

$$V_T''(R_B)=-\frac{D_C}{aR_N}\frac{J_0}{G_0}\left[1+0\left[\frac{a}{R_N}\right]\right]\equiv-\mu w_B^2\ . \tag{A7}$$

The pocket where V_T becomes a minimum can be similarly treated remembering that R_P is a bit smaller than R_N.

[1]A. Scalia, Nuovo Cimento **A92**, 210 (1986).
[2]T. Udagawa, B. T. Kim, and T. Tamura, Phys. Rev. C **32**, 124 (1985).
[3]G. Bertsch, Z. Phys. A **289**, 103 (1978).
[4]P. Braun-Munzinger and G. M. Berkowitz, Phys. Lett. **125B**, 19 (1983).
[5]B. Sahu and C. S. Shastry, Phys. Rev. C **38**, 1262 (1988).
[6]R. W. Hasse, Rep. Prog. Phys. **41**, 1027 (1978).
[7]J. N. Dey, Phys. Lett. **66B**, 315 (1977); S. K. Samaddar and M. I. Sobel, *ibid.* **88B**, 43 (1979); D. H. E. Gross, R. C. Nayak, and L. Satpathy, Z. Phys. **A299**, 63 (1981).
[8]S. N. Mukherjee and L. N. Pandey, Phys. Rev. C **28**, 1104 (1983).
[9]R. Bass, Nucl. Phys. **A231**, 45 (1974).
[10]J. Randrup, Ann. Phys. (N.Y.) **112**, 356 (1973); Nucl. Phys. **A327**, 490 (1979).
[11]D. H. E. Gross, in *Heavy-Ion, High Spin States and Nuclear Structure* (IAEA, Trieste, 1975), Vol. I, p. 27.
[12]K. Sivek-Wilczynska and J. Wilczynski, Nucl. Phys. **A264**, 115 (1976).
[13]G. Wolschin and W. Nörenberg, Z. Phys. A **284**, 209 (1978).
[14]B. Sahu and C. S. Shastry, J. Phys. G (in press).
[15]R. Bass, *Nuclear Reactions with Heavy Ions* (Springer-Verlag, Berlin, 1980), p. 235.